BIUST Research and Innovation Symposium 2019 (RDAIS 2019)
Botswana International University of Science and Technology
Palapye, Botswana, 4 - 7 June 2019
ISSN: 2521-2292

Lamellipodial Motility of a squared shaped cell - mathematical model

Matlhogonolo Rakakae[1] and Sachin Shaw[1]
[1]Department of Mathematics and Statistical Sciences,
Botswana International University of Science and Technology, Private Bag 16, Palapye, Botswana

Abstract

Cell motility is an important biological action in the creation, operation and maintenance of our bodies. One of the best studied types of motility is the lamellipodial motility on flat, hard and sticky surface. To advance our understanding of this essential biological process, it is necessary to develop a mathematical model explaining cell motility. We have considered the turning behavior and dependence of the motile behavior on the model parameters and boundary conditions of 2D square shaped cells. The model consists of force-balance and myosin transport equations which solved numerically by using finite difference method in MATLAB after nondimensionalized the governing equations along with initial and boundary conditions. The model analysis shows that initiation of motility critically depends on four dimensionless parameter combinations which represent the myosin contractility, characteristic viscosity-adhesion length, effective velocity and local boundary velocity. By simulating numerically a minimal free-boundary model we observed that cells are stationary when contractility is weak and motile behavior of a cell is sensitive to conditions of force balance at the cell boundary.

1 INTRODUCTION

Biofluid mechanics is the study of certain class of biological problems from fluid mechanics point of view [1]. In this article we will be focussing on the shape and movements of a motile cell undergoing lamellipodial motility. Cellular motility is the spontaneous movement of a cell from one location to another by consumption of energy. It encompasses several types of motion, including swimming, crawling, gliding and swarming. It is a fundamental biological phenomenon that underlies many physiological processes in health and disease, including wound healing, embryo genesis, immune response and metastatic spread of cancer cells, to name a few [2].

Many important physiological processes during development, such as cell migration during gastrulation, axon guidance, tissue regeneration and embryological development require Cell motility to happen. Unregulated cell migration can be the cause for progression of cancer, for example during metastasis.

Cell migration can have a more sinister role which is secondary tumour growth that is caused by a cancer cellâAZs ability to migrate from a primary tumour into the lymphatic system (plays a key role in the immune system, fluid balance, and absorption of fats and fat-soluble nutrients), eventually taking up residence at an alternate location. Deficiencies in the proteins associated with cell motility during foetal development have also been implicated in diseases such as spinabifida (malformed vertebrae). Obviously, a strong understanding is needed of cell motility and the constituents, which control this process [3].

Cell motility is an important biological action in the creation, operation and maintenance of our bodies. To advance our understanding of

ISSN: 2521-2292

this essential biological process, mathematical models explaining cell motility have to be developed [4]. With accurate models it is possible to explore many permutations of the same event and concisely investigate their outcome [5].

One of the best studied types of motility is the lamellipodial motility on flat, hard and sticky surface. Lamellipodia are ribbon-like flat cellular protrusions that are formed at the boundary (outer edge) of a moving or spreading cell. Lamellipodia are enriched with a bidimensional nerve fibre array of a branched network of actin filament [4].

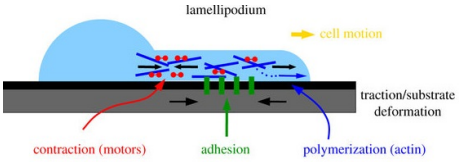

Figure 1: Illustration of the main physical mechanisms responsible for substrate-based cellular motion: actin polymerisation, substrate adhesion and contraction by molecular motors [4]

In Figure1, a thin sheet of actin filaments that stretches out to the cell's boundary, lamellipodia generate pushing forces that drive the cell forward. Micro-tubules can barely penetrate this actin network, but they direct cell motility in other ways, such as controlling cell adhesion and acting as the cell's internal compass. Adhesion exerts a powerful influence on a cell's behavior, controlling not only motility and structure but also growth and survival [6]. The following Figure 2 shows in detail how a cell moves with its lamellipodium.

Figure 2 explains the mechanisms involved in cell movement. There are three principal mechanisms that enable the keratocyte motility (keratocyte are erythrocytes with one or two projections that may form as a result of rupture of a vacuole or hole within an erythrocyte).
First, after determining its direction of motion, the cell extends a protrusion in this direction by actin polymerization at the leading edge. Secondly, it then attaches its leading edge to the surface on which it is moving and detaches at the cell body and rear. Finally, it pulls the whole cell body forward by contractile forces generated at the cell body and rear of the cell. Optimal adhesion strength for fast cell migration has been shown to depend on the level of myosin contraction [5].

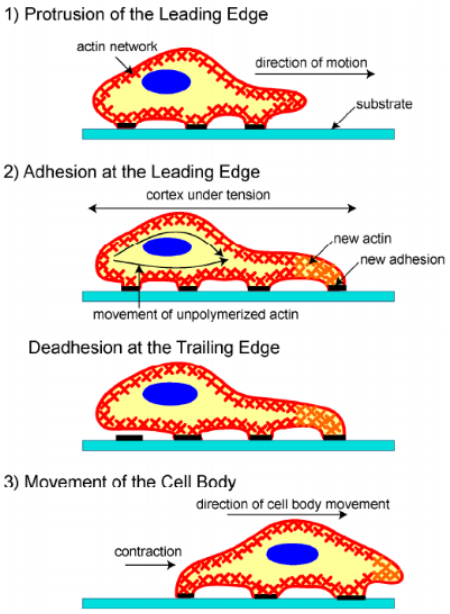

Figure 2: A schematic of the three stages of cell movement[6].

The corneal keratocytes (found on the surface of the cornea) shown in Figure 3 adopt distinct shapes dictated by adhesion onto surfaces coated with fibronectin (an extracellular matrix protein that anchors cells by binding adhesion receptors) [8]. These Keratocytes are composed of a highly elaborate polymer network, primarily actin filaments, which contract by the precise

ISSN: 2521-2292

alignment and binding of molecular motors. This type of contraction underlies the mechanical function of the cornea, but also the crawling and migration of other cells [9]. In this project we will be focused on the square shaped cell, bottom left.

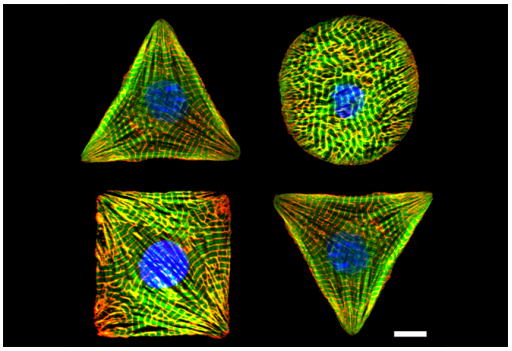

Figure 3: corneal keratocytes derived from embryonic stem cells[7]

The model in this project will predict the turning behavior and dependence of the motile behavior on the model parameters and boundary conditions of 2D rectangular shaped cells. We do this by simulating numerically a minimal free-boundary model by finding that
1) cells are stationary when contractility is weak
2) motile behavior of a cell is sensitive to conditions of force balance at the cell boundary [10].

2 MODELS AND METHODS

As stated previously Mechanics plays a dominant role in keratocyte motility. We concentrate on the second and last principal mechanism that enables keratocyte motility. The model consists of force-balance and myosin transport equations,

$$\eta \frac{\partial^2 U}{\partial X} + \sigma \frac{\partial M}{\partial X} - \xi U = 0\,, \qquad (1)$$

$$\frac{\partial M}{\partial T} = \frac{\partial}{\partial X}\left(D_{eff} \cdot \frac{\partial M}{\partial X} - U_{eff} M \right) \qquad (2)$$

For the velocity of actin flow **U**(X,t) and myosin concentration **M**(X,t) defined locally for $X \in \Psi(t)$, where $\Psi(t)$ is a moving 2D domain representing cell geometry. For the Force balance equation, equation (1);
• The first term describes the force due to passive viscous stresses in the deforming actin network where $\boldsymbol{\eta}$ is the effective actin viscosity [8]. We assume that the actin polymer mesh is compressible, so there is no incompressible condition.
• The second term describes the divergence of the myosin contractile stress. We assume the stress to be isotropic (exhibiting properties with the same values when measured along axes in all directions) and proportional to the myosin density, with $\boldsymbol{s}$ denoting the force per unit of myosin density.
• The third term describes the effective viscous drag arising from creeping movement of Filamentous actin (Factin;essential part of the cytoskeleton and build up many higher order structures in cells e.g. lamellipodia) relative to a substrate and characterized by the viscous drag coefficient $\boldsymbol{\xi}$ [10].
For the myosin transport,equation (2);
Kinetics of myosin can be interpreted in terms of transitions between two states:
• state of free myosin diffusing in the cytoplasm
• state in which myosin is bound to the actin network [11].

Clusters of the bound myosin contract the actin network and move with it. For low viscosity and slow diffusion, however, using U as an advection (movement of some material by the velocity of the fluid) velocity and constant diffusion coefficient (D) results in singular solutions, in which M and U develop Dirac-delta singularities [8]. The singular solutions are obviously unrealistic, given that myosin molecules have a finite size [12].

ISSN: 2521-2292

By introducing effective velocities which approach zero as $M \to M_{max}$ then the excluded volume effect can be taken into account [13] $\mathbf{U}_{eff} = \mathbf{U}(1 - M / M_{max,u})$.

Normally, in a free boundary problem, the actual maximum of myosin concentrations may significantly exceed the $M_{max,u.}$ This is because myosin accumulates at the rear of the cell where it is swept forward by a moving boundary and it only happens in motile solutions. This effect originates from the Rankine-Hugoniot boundary condition which describes the relationship between the states on both sides of a shock wave or a combustion wave (detonation) in a one-dimensional flow in fluids [9]. Hence, the effect of molecular crowding on myosin velocity should generally be written as;

$$\mathbf{U} = \begin{cases} \mathbf{U}(1 - M / M_{max,u}), & \text{if} \quad M < M_{max,u}, \\ 0 & \text{, Otherwise.} \end{cases}$$

As diffusion is also affected by crowding, then we have the effective diffusion which is given by $\mathbf{D}_{eff} = \mathbf{D}(1 - M/M_{max,d})$ with a value of the cut-off $M_{max,d}$ that exceeds the actual maximal densities of myosin [10].

2.1 Boundary Conditions

$$\mathbf{n}\cdot(\alpha\nabla\mathbf{u} + \beta m\mathbf{I})_{|\partial\omega(t)} = 0, \quad (3)$$

$$\mathbf{n}\cdot(-D_{eff}\nabla_x M + (\mathbf{U}_{eff} - \mathbf{V}_f)M)|_{\partial\omega(t)} = 0, \quad (4)$$

Equation (7), a diffusion-advection equation for myosin, is subject to the mass-on serving zero flux boundary equation (3), producing an additional dimensionless parameter,

$$\mu_{tot} = \int\int_{\omega(t)} m \cdot d\,|\omega|.$$

Also, for equation (8) its dimensionless boundary conditions are $\mathbf{u}|_{\partial\omega(t)} = 0$ and equation (4) Note that the varying parameter $k = KL^3D^{-1}$ is equivalent to re-scaling the actin polymerization constant. In addition, because the myosin contractility constant ß enters equation (8) with m, varying ß is similar to re-scaling μ_{tot} [10].

Cell becomes motile when myosin contractility is high [8] therefore we focus on the role played by four essential independent model parameters; v_f, μ_{tot}, α and u_{eff}.

2.2 Initial Conditions

$$u(x,0) = 0, \quad (5)$$

$$m(x,0) = (\mu_{tot}/|w|)(1 - gx), \quad (6)$$

By solving Equations (7) and (8) in domains with free boundaries steady dynamics of a motile cell were explored. Even though the force-balance equation does not involve time derivatives, the coupled system (7) and (8) constitutes an initial-value problem and one must specify initial conditions for both variables and the domain, ***m*(x,** 0), **u(x,** 0), and ***ω***(0) [10]. Initial conditions based on a stationary steady state in a rectangular geometry were used to clarify Equations (7) and (8) in domains with free boundaries.

2.3 Non-Dimensionalization

To nondimensionalize the model, we use the following set of units. The length unit L is defined as a characteristic linear size of the cell with a target area,

$$L = \sqrt{A_0/\pi}$$

Then the dimensionless variables, differential operator, and current and target cell areas are, respectively, $t = TD/L$.

$$t = TD/L, x = X/L, u = UL/D, m = M/M_0,$$

$$|\omega| = \frac{\Psi}{L^2}, a_0 = \frac{A_0}{L^2}$$

By using the above non dimensionalized parameter equation (1) and equation (2) reduces to:

$$\frac{\partial m}{\partial t} = \frac{\partial}{\partial x}\left(d_{eff}\frac{\partial m}{\partial x} - u_{eff}\,m\right), \quad (7)$$

$$0 = \alpha\frac{\partial^2 u}{\partial x^2} + \beta\frac{\partial m}{\partial x} - u, \quad (8)$$

where $u_{eff} = u(1 - m/m_{max,u})$, if $m < m_{max,u}$, and zero otherwise, and $d_{eff} = 1 -$

ISSN: 2521-2292

$m/m_{max,d}$. Equation (8) include two dimensionless parameters:

• the dimensionless viscosity-adhesion length parameter $a = n/L^2\xi$,

• the myosin contractility constant $\beta = \sigma M_0 / D\xi$.

The viscosity-adhesion parameter $\boldsymbol{a}$ is the ratio of the length scale of the mechanical action of the cell size, since the mechanical effect of localised myosin contraction spreads on the length scale $\sqrt{\eta/\xi}$ [10].

2.4 Numerical Techniques

From our equations (7) and (8) we simplify them using the finite difference method;

$$\alpha\Delta u_{n+1}^{k+1} + \beta\nabla m_n^{k+1} - u_{n+1}^{k+1} = 0,$$

(9)

$$\alpha\left(\frac{u_{j+1} - 2u_j + u_{j-1}}{(\Delta x)^2}\right) + \beta\left(\frac{m_{j+1} - m_{j-1}}{2\Delta x}\right) - \frac{1}{2}\left(u_{j+1} + u_{j-1}\right) = 0,$$

(10)

and

$$\partial_t m = \nabla\cdot(d_{eff}\nabla m - u_{eff} m) = d_{eff}\Delta m - u_{eff}\nabla m,$$

(11)

$$\frac{m_{j+1} - m_{j-1}}{2\Delta t} = d_{eff}\left(\frac{m_{j+1} - 2m_j + m_{j-1}}{(\Delta x)^2}\right) - u_{eff}\left(\frac{m_{j+1} - m_{j-1}}{2\Delta x}\right),$$

(12)

thus the following Thomas algorithm values are obtained; for equation (7) we get;

$$u_{diag} = \left(\frac{d_{eff}}{(\Delta x)^2} - \frac{u_{eff}}{\Delta x} - \frac{1}{2\Delta t}\right),$$

$$\text{diag} = \left(\frac{-2}{(\Delta x)^2}\right),$$

$$l_{diag} = \left(\frac{d_{eff}}{(\Delta x)^2} - \frac{u_{eff}}{\Delta x} + \frac{1}{2\Delta t}\right),$$

rhs = 0.

for equation (8) we get;

$$u_{diag} = \left(\frac{\alpha}{(\Delta x)^2} - \frac{1}{2}\right),$$

$$\text{diag} = \left(\frac{-2\alpha}{(\Delta x)^2}\right),$$

$$l_{diag} = \left(\frac{\alpha}{(\Delta x)^2} - \frac{1}{2}\right),$$

$$rhs = \frac{\beta}{2\Delta x}\left(m_{j+1}^k - m_{j-1}^k\right).$$

Second, the system equations (7) and (8), consists of the parabolic and linear equations, since were are dealing with a rectangular cell. The equations are coupled via the advection term of the parabolic equation and myosin dependent stress term in the linear equation, as well as through the boundary conditions at the moving boundary; also, the effective transport parameters are functions of the myosin concentration. To solve the system, we implemented a segregated solution strategy i.e (used the finite difference method in matlab), in which equations are solved one at a time and nonlinear terms are treated by fixed point iterations. One advantage of the segregated solver is that it prevents the matrix of a linearized system from becoming very large even with very fine computational grids [1]. The algorithm is illustrated below for one time step by the mathematical pseudo-code. In simple terms, Matlab was used to obtain the result.

- initial conditions
- boundary conditions
- set $m_1^{k+1} = m^k$ and $u_1^{k+1} = u^k$

for $n = 1: MaxNumIters$

- solve $\alpha\Delta u_{n+1}^{k+1} + \beta\nabla m_n^{k+1} - u_{n+1}^{k+1} = 0$ to get u_1^{k+1}
- evaluate u_{eff} and d_{eff} using $u_1^{k+1} = u^k$ and $m_1^{k+1} = m^k$.

-solve $\left(m_{n+1}^{k+1} - m^k\right)/\Delta t = \nabla\cdot\left(d_{eff}\nabla m_{n+1}^{k+1} - u_{eff} m_{n+1}^{k+1}\right)$ to get m_{n+1}^{k+1}.

ISSN: 2521-2292

-calculate absolute errors

$\| u_{n+1}^{k+1} - u_n^{k+1} \|_\infty$ and $\| m_{n+1}^{k+1} - m_n^{k+1} \|_\infty$.

- if solution converged, break the loop, else $m_n^{k+1} = m_{n+1}^{k+1}$, $u_n^{k+1} = u_{n+1}^{k+1}$ end of segregated loop.

If $n = 1 : MaxNumIters$ $m_n^{k+1} = m_{n+1}^{k+1}$, $u_n^{k+1} = u_{n+1}^{k+1}$, else iterations are stagnant.

Where MaxNumIters is the maximum allowed number of iterations. [10]

3 RESULTS AND DISCUSSION

3.1 Difference of myosin concentration and velocity with respect to varied effective velocity

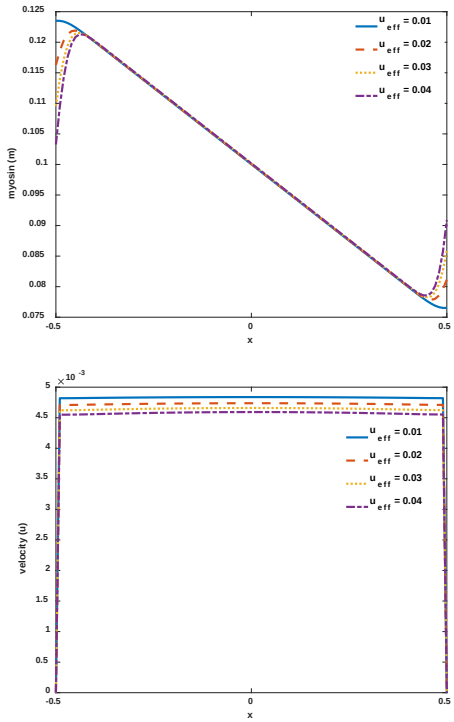

Figure 4: describes how the myosin concentration and velocity changes when the effective velocity is varied.

The myosin concentration model generally predicts significantly higher cell speeds compared to those in the velocity model (Figure 4). This is because in the myosin concentration model, the fast linear flows of cells generated by myosin at the rear boundary tend to decrease the cell area, leading to fast effective protrusion at the front [8]. As a result, as the cell area decreases with total myosin the cell speed increases. Interestingly, the cell speed in the velocity model decreases slightly as the effective velocity increases, which can be understood by noting that the cell area in this model increases with effective velocity, thus weakening the effect of myosin.

3.2 Difference of myosin concentration and velocity with respect to varied local boundary velocity

For figure 5, as the local boundary velocity is increases the myosin concentration model decreases steadily and the velocity increases as x increases. This means that as myosin relocates to the boundary, because of the zero actin velocities at the boundary. An initially small, local maximum of myosin (m) that appears at the boundary point closest the main maximum (*m*) due to slightly faster diffusion. Thus, the competition between the two maxima lowers the myosin gradients on one side of the cell, resulting in a net force acting on it in that direction [10]. Hence, resulting in the relocation of myosin. In the cell with a free boundary, the re-distribution of myosin is conferred to boundary velocity, resulting in slower outward and eventually inward movements of the part of the boundary that becomes the cell rear. The cell movement further skews the myosin towards the rear resulting in movement [10].

ISSN: 2521-2292

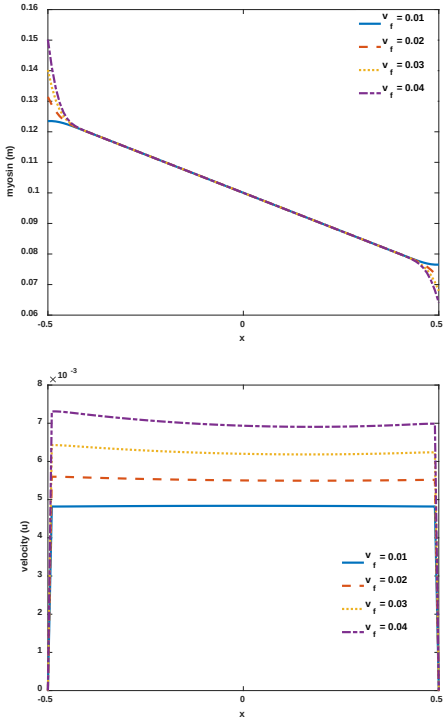

Figure 5: describes how the myosin concentration and velocity changes when the local boundary velocity is varied.

3.3 Difference of myosin concentration and velocity with respect to varied contractility parameter

As the myosin concentration and the velocity increases as shown in Figure6, the contractility also increases. That is, the contractile forces generating linear flow of myosin, are proportional to the myosin gradients which in turn, are reinforced by advection of myosin. Initiation of motility in the free-boundary models is driven by competition between the myosin contractile stress and dissipative processes (a process in which energy e.g. internal, bulk flow kinetic, or system potential, is transformed from some initial form to some final form) [10]. Motility occurs when the contractility prevails over the dissipation (a process in which energy is used or lost without accomplishing useful work) [8]. In the limit of large values of ***a***, the actin network is effectively stiff and thus does not allow for significant actin flows, thus making the cell less motile and slower. This is why the velocity goes to zero as the cell becomes less motile.

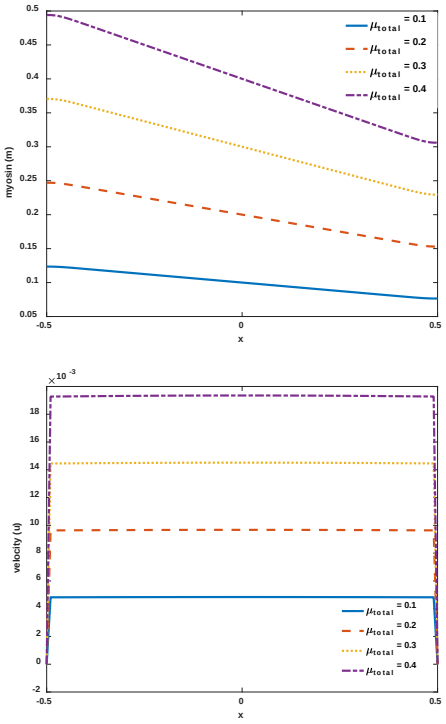

Figure 6: describes how the myosin concentration and velocity changes when the contractility parameter is varied.

3.4 Difference of myosin concentration and velocity with respect to varied cell viscosity-adhesion length

An increase in the cell viscosity-adhesion length (***a***) results in a significant in the myosin model, whereas the velocity model increases drastically. This is because for the large viscosity-adhesion length, the actin

ISSN: 2521-2292

network becomes very flexible at first and eventually becomes stiff after some time.

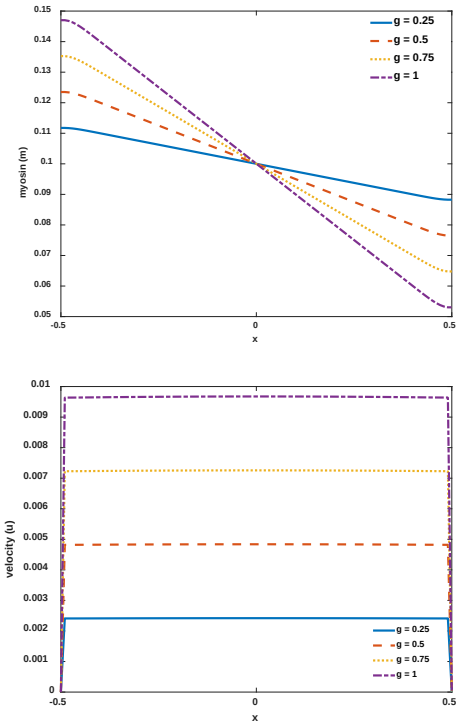

Figure 7: describes how the myosin concentration and velocity changes when the cell length is varied.

Thus, does not allow for significant actin flows, which makes the cell more symmetric and as a consequence less motile and slower, this is why the velocity model graphs approach zero eventually. So in the limit of very large values of viscosity- adhesion lengths, the cell is stationary, the same argument has been enforced by Etienne et al., [14]. In case of short viscosity-adhesion lengths, myosin forms a very small high-density aggregate, which affects the actin network only locally [10]. In this case, the steady motility is impossible and the cell starts to turn.

4 CONCLUSION

In this project, we explored the ability of a minimal actin-myosin contractility model [15] to reproduce observed mechanical states of the simplest motile cell. The model analysis has shown that the mechanical state of the cell critically depends on just four dimensionless parameters representing the myosin contractility, characteristic viscosity adhesion length, effective velocity and local boundary velocity. For the large viscosity-adhesion length, the actin network eventually becomes stiff and does not allow for significant actin flows, which makes the cell less motile and slower, and as a consequence the cell is becomes stationary. For short viscosity-adhesion lengths, steady motility is impossible, and the cell starts to turn. In conclusion, it can be said that for a cell to move straight and steadily, it has to keep the viscosity adhesion length on the order [14]. Intuitively, if myosin contractility is weak, the myosin spreads uniformly and the cell remains stationary and symmetric. The mode of motility depends on the boundary conditions [8]. For the zero actin velocity at the boundary and the sufficiently small actin growth constant and cell speed. The main finding of my study is that the contractile mechanism of motility results in a very strong turning behavior of the cell. Similarly, the model predicts that the lamellipodial area increases at lower myosin contractility, and that the cell speed increases with myosin contractility. Lastly, higher myosin contractility are predicted to promote the cell polarization and motility initiation [10]. Keratocyte motility and steady shape of the moving cell inspired a great deal of free boundary modeling in the past decade [15]. So in conclusion, mechanical force balance determines cell shape and movements.

References

[1] Jagan N. Mazumdar. Biofluid Mechanics. World Scientific Publishing

ISSN: 2521-2292

Co Pte Ltd, South Australia, 1992.
[2] Burridge K Firtel RA Ginsberg MH Borisy G Ridley AJ, Schwartz MA. Cell migration:. integrating signals from front to back, 302:1704–1709, 2003.
[3]P.E. McHugh Brendan Flaherty, J.P. McGarry. Cell biochemistry and biophysics. Mathematical models in cell motility, 49:14–28, 2007.
[4]Irina Kaverina Alissa M.Weaver Bong HwanSung, Xiaodong Zhu. Current biology, Cortactin Controls Cel l Motility and Lamellipodial Dynamics by Regulating ECM Secretion, 21:1460–1469, 2011.
[5] Alexander Mogilner Noa Ofer and Kinneret Keren. Plos biology,. Actin disassembly clock determines shape and speed of lamellipodial fragments,, 108:20394–20399, 2011.
[6] Revathi Ananthakrishnan and Allen Ehrlicher. International journal of biological sciences. The Forces Behind Cell Movement, 3(5):303–317, 2017.
[7] Yvonne S. Aratyn Kevin Kit Parker Francesco S. Pasqualini, Josue A Goss. I Heart Actin, 2009.
[8]Jacobson K Verkhovsky AB Mogilner A. Rubinstein B, Fournier MF. Biophys j. Actin-Myosin Viscoelastic Flow in the Keratocyte Lamellipod,, 101:545–553, 2011.
[9] Wazir Muhammad Ijaz Ali Peter Bastian Muhammad Sabir, Abdullah Shah. Computers and mathematics with applications. A mathematical model of tumor hypoxia targeting in cancer treatment and its numerical simulation, 74:3250–3259, 2017.
[10] Stephanie Pulford Aaron Rumack Jamie Brandon Boris M. Slepchenko Alex Mogilner Masoud Nickaeen, Igor L. Novak. Plos computational biology, A free-boundary model of a motile cell explains turning behavior,, 13, 2017,.
[11]S. Praetorius W. Marth and A. Voigt. Physica d. A mechanism for cell motility by active polar gels, 12(107), 2015.
[12]Yoshimi Takai Yoshiyuki Rikitake. International review of cell and molecular biology,. Directional cell migration regulation by small G proteins, nectinlike molecule-5 and afadin,, 287:97–143, 2011.
[13]Michal O. Nowicki E. Antonio Chiocca Avner Friedman Yangjin Kim, Sean Lawler. Journal of theoretical biology. A mathematical model for pattern formation of glioma cells outside the tumor spheroid core, 260:359–371, 2009.
[14]DÃlmosthÃlne Mitrossilis Nathalie Bufi Pauline Durand-Smet Jocelyn ÃLtienne, Jonathan Fouchard and Atef Asnacios. Pnas. Cells as liquid motors: Mechanosensitivity emerges from col-lective dynamics of actomyosin cortex, 112(9):2740–2745, 2015.
[15]Allen G.M. Theriot J.A. Mogliner A. Barnhart EL, Lee KC. Proc natl acad sci. Balance between cell-substrate adhesion and myosin contraction determines the frequency of motility initiation in fish keratocytes, 112(16):5045–5050, 2015.